Automatic Measurement Technique of Electromagnetic Rotation in a Nonreciprocal Medium

Swadesh Poddar, *Member, IEEE*, Alexander M. Holmes, *Member, IEEE*, and George W. Hanson, *Fellow, IEEE*

***Abstract*— Faraday rotation is a nonreciprocal rotation of wave polarization as a wave propagates. Faraday rotation is a critical property in a wide range of applications, from wireless communication to quantum memory, from bio-magnetic field detection to sensor applications. Characterizing the nonreciprocal polarization rotation accurately is very important for these applications. This article aims at developing a simple, automated test bench procedure based on simplified mathematical modeling to measure polarization rotation of an electromagnetic (EM) wave upon propagation through a nonreciprocal medium. A comprehensive measurement approach is developed from the scattering matrix. The proposed measurement procedure is demonstrated using an electronically tunable nonreciprocal metamaterial, and the accuracy of the proposed method is verified by comparison to the well-accepted conventional measurement technique, as well as 3-D EM simulation.**

***Index Terms*— Faraday rotation, metamaterial, nonreciprocity, polarization rotation, test bench.**

I. Introduction

POLARIZATION rotation, the change in orientation of the plane of polarization about the microwave/optical axis of a linearly polarized wave as it propagates through certain materials, is an important concept in both reciprocal and nonreciprocal systems. The precise determination of the polarization state of an electromagnetic (EM) wave is fundamental for a wide variety of applications in microwaves, radio frequency (RF) front ends, astronomy, optics, and terahertz technology, and remote sensing, to name just a few. A linearly polarized EM wave may be represented as the sum of two circularly polarized waves (right- and left-handed circular polarized waves) with opposite handedness and equal amplitude. Faraday rotation occurs when EM waves propagate through a nonreciprocal medium, whereupon the right-handed and left-handed circularly polarized waves (L/RHCP) propagate with different phase velocities, and experience different impedance and refractive indices. These LHCP and RHCP waves start to accumulate a phase difference as they propagate through the medium, therefore, with respect to time and distance, the direction of linear polarization changes. The greater the deviation in phase velocity, the greater the rotation [1], [2], [3].

The robust practical measurement of polarization rotation in a nonreciprocal medium is very challenging. Various approaches have been investigated to accurately measure Faraday rotation in various frequency regimes [4], [5], [6], [7], [8], [9], [10] and the most conventional approach is to measure polarization rotation by rotating an antenna [9]. However, manual approaches to measure Faraday rotation lack precision and are time-consuming. Therefore, a simple, realizable, cost-effective, accurate test-bench model is of immense importance to measure Faraday rotation. In this work, we have developed a simplified and automatic S-parameter translation to measure polarization rotation in a nonreciprocal environment using a network analyzer. We apply our proposed measurement method to one of our previously developed nonreciprocal metamaterials, and we observe good agreement with manual measurement. Furthermore, our proposed model will work for a nonreciprocal slab of finite thickness.

The article is organized as follows. In Section II, we provide insight to the mechanism of EM nonreciprocity and various polarization rotations, in Section III, we present the S parameter analysis leading to simplified automatic Faraday rotation measurement and, in Section IV, we benchmark our proposed measurement model with simulation and with a conventional approach on one of our previously implemented tunable nonreciprocal metasurfaces.

II. Electromagnetic Nonreciprocity and Polarization Rotation

A system can be subdivided into two broad categories based on its interaction with EM waves: reciprocal and nonreciprocal. A reciprocal system is one in which the fields created by the source at an observation point is the same when source and observation points exchange position, which can be represented by the scattering parameter equality, $\mathbf{S} = \mathbf{S}^{\mathbf{T}}$. Devices such as antennas, passive RLC electrical circuits, and most RF components are reciprocal. On the other hand, nonreciprocity, and the associated broken time reversal (TR)

Manuscript received 27 April 2022; revised 17 August 2022; accepted 31 August 2022. Date of publication 12 September 2022; date of current version 3 October 2022. This work was supported by the National Science Foundation under Grant EFMA1741673. The Associate Editor coordinating the review process was Zhengyu Peng. *(Corresponding author: Swadesh Poddar.)*

The authors are with the Department of Electrical Engineering, University of Wisconsin-Milwaukee, Milwaukee, WI 53201 USA (e-mail: poddarswadesh@gmail.com).

Digital Object Identifier 10.1109/TIM.2022.3205677

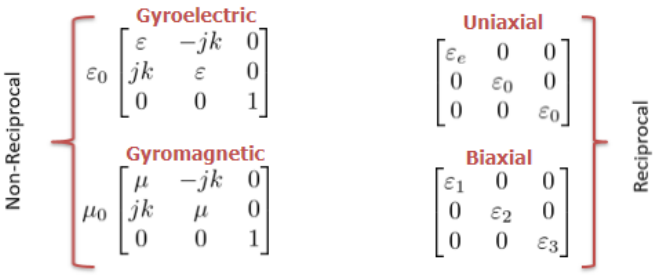

Fig. 1. Matrix representation of various media and classification of non-reciprocal and reciprocal media.

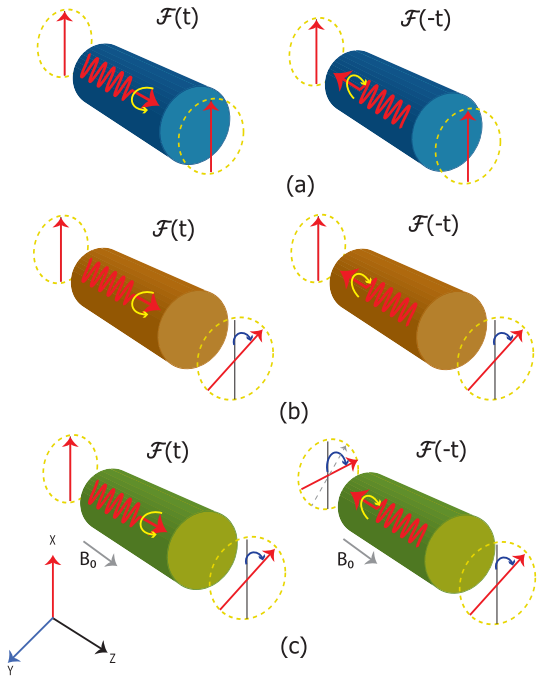

Fig. 2. Criteria for TRS and TR asymmetry. (a) Isotropic medium (b) Chiral medium (reciprocal). (c) Faraday system by unaltered external magnetic bias, hence, TRS breaking, an example of a nonreciprocal system.

symmetry, dictates that the field created by the source and measured at the observation point is different when source and observation points are interchanged, and can be represented by $\mathbf{S} \neq \mathbf{S}^{\mathbf{T}}$ [3], [11], [12]. As an example, nonreciprocal components such as gyrators, isolators, and circulators, are very important because of their impact on military applications, telecommunications, and so on [11], [13]. There are various reported approaches to that achieve nonreciprocity since the 1950s such as using ferrite materials biased by a static magnetic field, and the latest concept of achieving nonreciprocity using time modulation [12]. In all reported cases of achieving nonreciprocity, the fundamental concept is breaking TR symmetry (TRS) which is unassociated with loss [2], [3].

Polarization rotation is directly related to material properties, and system conditions. For example, polarization rotation in various material and structural systems, such as chiral materials, wire grid polarizers, ferrites, plasmas, birefringents, and gyrotropic mediums are different; polarization rotation may be reciprocal, or nonreciprocal. If a linearly polarized wave travels forward through a nonreciprocal medium by a distance l, gets reflected, and travels back to the starting point, the polarization rotation angle can be represented as [14]

$$\phi = \frac{1}{2}(k_+ - k_-)l \tag{1}$$

where wavenumber is $k_\pm = \omega\sqrt{\epsilon\mu_\pm}$, impedance is $\eta_\pm = (\mu_\pm/\epsilon)^{1/2}$ and permeability is $\mu_\pm = \mu_1 \pm \mu_2$. Therefore, the LHCP and RHCP waves exhibit different phases, impedances, and refractive indices.

Polarization rotation, the phase difference between cross polarized components, and transmission parameters (S_{21}, S_{12}) are key performance indicators to characterize nonreciprocity. For example, nonreciprocal gyrotropy is the usual way to achieve nonreciprocity via having a certain type of off-diagonal elements in the μ or ϵ tensor. Fig. 1 represents the matrix form of various reciprocal and nonreciprocal cases. In bulk media nonreciprocity requires asymmetric electric permittivity and magnetic permeability which can be classified as gyroelectric ($\varepsilon \neq \varepsilon^{\mathbf{T}}$) and gyromagnetic ($\mu \neq \mu^{\mathbf{T}}$), respectively, wherein Fig. 1, k in the off-diagonal terms represent the gyrotropic parameters. Nonreciprocal gyrotropic and gyromagnetic materials exhibit off-diagonal tensor elements, whereas, reciprocal cases such as uniaxial or biaxial material do not have any off-diagonal elements, hence, the gyrotropic response of the magnetized ferrites is evident. In addition, the presence of off-diagonal tensor components, and nonreciprocal materials exhibit cross polarized phase and magnitude difference [15]. It is important to note here that systems with symmetric tensors $\varepsilon = \varepsilon^{\mathbf{T}}$ or $\mu = \mu^{\mathbf{T}}$ with nonzero off-diagonal elements exhibit polarization rotation (optical activity), however, in a reciprocal way [16].

To characterize material interactions with EM waves, in Fig. 2 we show three different systems that can be classified with respect to TR symmetry and asymmetry [3]. Fig. 2(a) depicts an isotropic medium where there is not any polarization rotation and hence, is classified as reciprocal. Fig. 2(b) represents a chiral system, where the x polarized wave travels through the medium and experiences a polarization rotation of ϕ^0 at the receiver end, and if it reflects and travels in the reverse direction it will experience a polarization rotation of $-\phi^0$. As a result, the field polarization of a chiral system symmetrically returns to its original state, hence, this is a reciprocal system. Fig. 2(c) depicts Faraday rotation in the presence of a static $\mathbf{B}_0$ field. The applied static magnetic bias breaks time-reversal symmetry, making the process time-reversal asymmetric [2], [3], [17]. In comparison to the chiral case, the wave experiences ϕ^0 rotation, then in the reverse direction it experiences another ϕ^0 rotation, revealing Faraday rotation [18]. To recapitulate, the process of polarization rotation can be reciprocal or nonreciprocal. In the case of Faraday rotation, the sign (clockwise or anticlockwise) is determined relative to the axis along which TRS is broken, whereas, in chiral media exhibits reciprocal magneto-electric coupling, the sign of rotation is determined relative to the propagation direction [15], [19]. The next section will be

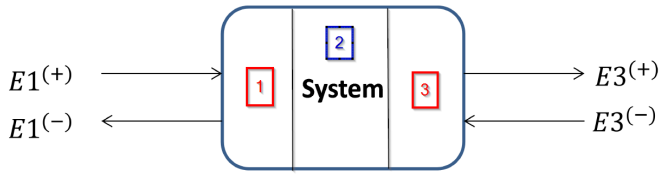

Fig. 3. Two-port network model where medium 1 and 3 are reciprocal and medium 2 is nonreciprocal.

focused on developing a realistic model for the measurement of polarization rotation in a transparent medium.

III. Principle of Operation and Practical Realization

Fig. 3 depicts a two-port network segmented into three parts used for our mathematical modeling of Faraday rotation, where segments 1 and 3 represent reciprocal media and segment 2 represents nonreciprocal media. Superscript +/− represents forward/backward waves. For practical realization, focus will be on measuring E_1^+, E_1^-, E_3^+, and E_3^- in terms of S matrices which can be represented by reflection and transmission components as

$$\vec{\mathbf{S}} = \begin{bmatrix} \vec{\mathbf{r}}^{(-)} & \vec{\mathbf{t}}^{(-)} \\ \vec{\mathbf{t}}^{(+)} & \vec{\mathbf{r}}^{(+)} \end{bmatrix} = \begin{bmatrix} \vec{\mathbf{S}}_{11} & \vec{\mathbf{S}}_{12} \\ \vec{\mathbf{S}}_{21} & \vec{\mathbf{S}}_{22} \end{bmatrix} \tag{2}$$

the arrow defines tensor components and $\vec{\mathbf{r}}$ and $\vec{\mathbf{t}}$ define the reflection and transmission tensors, respectively.

Therefore, (2) can be represented as

$$\vec{\mathbf{S}} = \begin{bmatrix} S_{11}^{yy} & S_{11}^{xy} & S_{12}^{yy} & S_{12}^{xy} \\ S_{11}^{yx} & S_{11}^{xx} & S_{12}^{yx} & S_{12}^{yy} \\ S_{21}^{yy} & S_{21}^{xy} & S_{RR}^{yy} & S_{22}^{xy} \\ S_{21}^{yx} & S_{21}^{xx} & S_{22}^{yx} & S_{22}^{yy} \end{bmatrix} \tag{3}$$

where the wave is being transmitted in the Z-direction and the first and second subscript/superscript represents port number/polarization of receiver and transmitter antenna, respectively. In our proposed transmission-based measurement, four S-parameter coefficients (i.e., S_{21}) are measured for different transmit polarizations. For example, the cross-polarized S-parameter S_{21}^{xy} (S_{21}^{yx}) is described as the transmission coefficient from antenna 1 to antenna 2 when the incident wave is $y(x)$ polarized and the received wave is $x(y)$ polarized. Similarly, the co-polarized S-parameter S_{21}^{yy} (S_{21}^{xx}) is described as the transmission coefficient from antenna 1 to antenna 2 when the incident wave is $y(x)$ polarized and the received wave is $y(x)$ polarized. We obtain Faraday rotation when the cross polarized transmission component from port 1 and port 2 are not the same. We can easily calculate Faraday rotation by using (4) as described in the Appendix [1], [20], [21], [22]

$$\theta_F = \frac{1}{2}\tan^{-1}\left(\frac{t_{\circlearrowleft\circlearrowleft}}{t_{\circlearrowright\circlearrowright}}\right) \tag{4}$$

where $t_{\circlearrowleft\circlearrowleft}$ defines the transmission component due to both incident waves from port 1 and received waves at port 2 being LHCP. Similarly, $t_{\circlearrowright\circlearrowright}$ defines the transmission component due to an incident and received waves being RHCP. Therefore, from (3) Faraday rotation can be represented in terms of S parameters in linear polarization as

$$\theta_F = \frac{1}{2}\tan^{-1}\left(\frac{S_{21}^{xx} + S_{21}^{yy} - i\left(S_{21}^{xy} - S_{21}^{yx}\right)}{S_{21}^{xx} + S_{21}^{yy} + i\left(S_{21}^{xy} - S_{21}^{yx}\right)}\right). \tag{5}$$

Fig. 4(a)–(d) depicts the various co-polarized and cross-polarized states of the receiver with respect to the transmitter, while Fig. 4(e)–(h) shows the measured S-parameters associated with each case in Fig. 4(a)–(d), respectively. From the measurement, it is clear that the co-polarized measurements Fig. 4(e) and (g) show very little sign of isolation while the cross-polarized measurements Fig. 4(f)–(h) exhibit a large amount of isolation at the resonant frequency. A major challenge in measuring Faraday rotation is that while the transmission is maximum at resonance, it is still very low. To account for Faraday rotation accurately, the signal from antenna 1 to antenna 2 and vice versa must pass through the metasurface only. As a result, the metasurface at a far-field distance from both antennas must be sufficiently large. Furthermore, when the transmission coefficients are very weak, the diffraction on the edges might be comparable or even greater than the desirable transmitted signal which affects the measurements. To quantify if edge effects are present, the metasurface can be repositioned in the xy plane (keeping it in-plane, at the same distance to the antenna) and if these small lateral movements do not change the results, then no edge effects are likely to present. In summary, careful consideration of test bench setup, calibration, and surrounding environment is very important to measure transmission-based nonreciprocal polarization rotation. Once the co-polarized and cross-polarized S-parameter coefficients are measured, an in-house script is used to compute Faraday rotation calculation with respect to frequency using (5).

IV. Simulation and Measurement

In our previous work [23], we calculated and measured the Faraday rotation of a normally incident plane wave on an electronically tunable nonreciprocal metasurface. Tunable nonreciprocity in the metasurface was introduced using a field effect transistor (FET) with variable gate–source and drain–source bias conditions. Here, we elaborate on the measurement procedure used in [23], and show agreement between the calculated and manually measured results for a set bias condition where the drain–source current is saturated.

Fig. 5 shows a block diagram of the measurement procedure to calculate Faraday rotation from the measured S-parameters over the operational frequency range. The diagram depicts the fabricated metasurface placed equidistant between the antennas, in the minimum required far-field. A 30V 5A HY3005F-3 linear dc power supply is used to bias the metasurface. Once the mechanical setup and calibration (S-Short, O-Open, L-Load, T-Through) of the Keysight E8361 vector network analyzer (VNA) is completed, a measurement is performed to obtain the co-polarized and cross-polarized S-parameter coefficients, which are then fed into (5) to calculate Faraday rotation with respect to operating frequency. A nonreciprocal system will exhibit a phase difference in the cross-polarization,

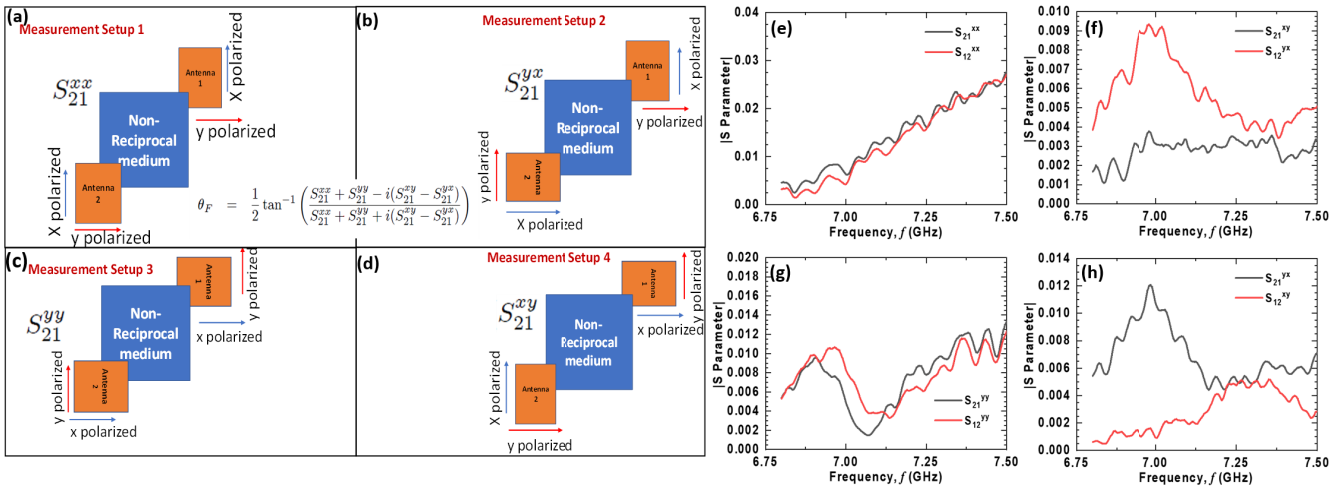

Fig. 4. (a)–(d) Automatic Faraday rotation measurement in four steps leading to combined numerical calculation (left). (e)–(h) Measured S-parameter spectra for Co-Pol and Cross-Pol configurations used to calculate Faraday rotation.

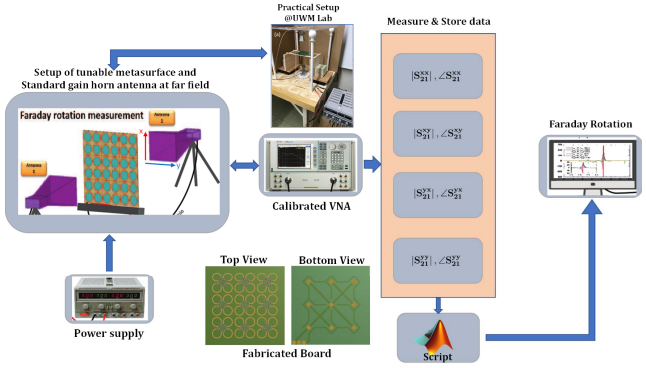

Fig. 5. Process flow of proposed automatic Faraday rotation as a function of frequency.

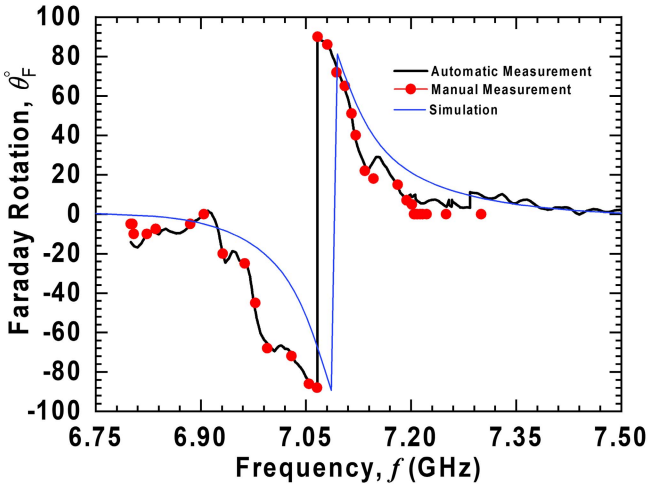

Fig. 6. Measurement of Faraday rotation based on automatic and manual process and comparison with simulation.

however, the co-polarized states exhibit no phase difference. This principle holds for both Faraday (transmission-based) and Kerr (reflection-based) rotation [15], [23].

For comparison, a manual method to measure Faraday rotation at different operating frequency points can be used (see [23] for details regarding the measurement setup). Fig. 6 shows the measured Faraday rotation obtained using the automatic (calculated) and manual measurement with respect to the frequency range of operation. Besides, for benchmarking, we have compared our measured results with simulation [23]. We achieve a very good agreement between simulation, manual measurement, and proposed automatic measurement. The slight resonance shift between simulation and measurement is due to the dielectric permittivity shift at a high frequency of the material (fr4) from its nominal catalog value we have used in the metasurface simulation. To measure the Faraday rotation, the conventional approach is to rotate the receiving antenna until maximum transmission (i.e., maximum $|S_{21}|$ or $|S_{12}|$) is achieved, which we are calling manual measurement in the literature. Furthermore, a detailed model validation has been described in Appendix B.

TABLE I
COMPARISON OF THE RECENTLY PROPOSED MEASUREMENT OF NONRECIPROCAL POLARIZATION ROTATION

Criteria	[10]	[9]	[7]	This Work
Measurement Type	Discrete	Discrete	Continuous	Continuous
Setup	Open Space	Open Space	Waveguide	Open Space
Measured Component	Transmission	Reflection	Transmission	Transmission
Measured Co-Cross Pol	No	No	Not Reported	Yes
Process	Automatic (Interpolation)	Manual	Automatic (Back-fitting)	Automatic
Tunability	Full scale	Partial	Full Scale	Full Scale
Bias	Magnetic	Electronic	Magnetic	Electronic

Table I compares/contrasts the proposed method with the various other methods of measuring Faraday rotation reported by researchers over the last years. Parsa *et al.* [10] proposed

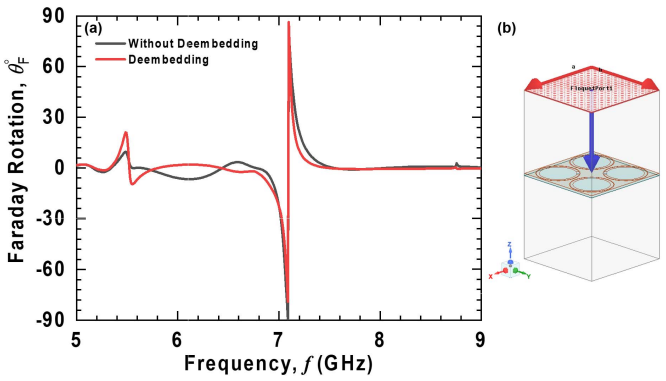

Fig. 7. (a) Comparative analysis of deembedding impact on Faraday rotation. (b) Simulation setup with floquet port and deembedding option active, the arrow direction from port to metasurface define the deembedding distance.

two measurement setup of nonreciprocal polarization rotation in nickel nanowires where they measured Faraday rotation with respect to various applied magnetic field. The first set of experiments was performed to confirm the existence of Faraday rotation in the material under test (MUT) and in the second set of experiments, birefringence was eliminated by employing quasi-optical components and the Faraday rotation angle was calculated using Mueller matrix. Proposed setup requires a number of apparatuses such as lens, polarizing filter, beam splitter, antennas, spherical mirror and offers measurement of Faraday rotation over discrete points. Kodera *et al.* [9] measured Faraday rotation in various electronic bias condition. Their proposed method is based on the reflected wave from the surface of the device under test (DUT) [9]. Both receiving and transmitting antennas need to be placed on the same side of the metasurface and they measured nonreciprocal polarization rotation based on rotating the antenna. Sounas *et al.* [7] proposed a waveguide-based measurement method where they extracted Faraday rotation with respect to various applied magnetic biases. They used graphene on a quartz substrate which is inserted in the middle of a circular waveguide, connected to two identical rectangular-coaxial adapters through circular-rectangular transitions where the bottom transition is rotated by an angle with respect to the top one. In comparison with other works, our proposed measurement procedure offers a very simple, cost-effective, precise measurement of polarization rotation and can be applied to the DUT of various dimension. In addition, in our proposed model we can calculate Faraday rotation over all frequencies whereas most of the conventional approaches are based on manual measurement of Faraday rotation by rotating the receiving antenna at various frequency points and post interpolation between those discrete data points which lacks the resolution to assess important details.

V. Conclusion

To summarize, we have presented an S-parameter model leading to a very simple and accurate test-bench setup to measure polarization rotation in an anisotropic medium using our previously designed nonreciprocal metasurface. The numerical modeling has been analyzed and verified. We envision that this proposed model will add a new building block in the measurement of polarization rotation and can be implemented in different types of polarization rotation systems utilizing two linearly polarized antennas and a network analyzer.

Appendix A
Mapping Between Transmission Matrix in Linear and Circular Basis

The transmission matrix on a linear basis can be mapped to a transmission matrix on a circular basis by following the advanced Jones calculus [24] as

$$\begin{bmatrix} \mathbf{t}_{\circlearrowright\circlearrowright} & \mathbf{t}_{\circlearrowright\circlearrowleft} \\ \mathbf{t}_{\circlearrowleft\circlearrowright} & \mathbf{t}_{\circlearrowleft\circlearrowleft} \end{bmatrix} = \frac{1}{2}\begin{bmatrix} P & Q \\ R & S \end{bmatrix} \tag{6}$$

where

$$\begin{aligned} P &= t_{xx} + t_{yy} + i(t_{xy} - t_{yx}) \\ Q &= t_{xx} - t_{yy} - i(t_{xy} + t_{yx}) \\ R &= t_{xx} - t_{yy} + i(t_{xy} + t_{yx}) \\ S &= t_{xx} + t_{yy} - i(t_{xy} - t_{yx}) \end{aligned}$$

and $\mathbf{t}_{\circlearrowright\circlearrowright}$ = Incident RHCP to recieved RHCP, $\mathbf{t}_{\circlearrowright\circlearrowleft}$ = Incident LHCP to recieved RHCP, $\mathbf{t}_{\circlearrowleft\circlearrowright}$ = Incident RHCP to recieved LHCP, and $\mathbf{t}_{\circlearrowleft\circlearrowleft}$ = Incident LHCP to recieved LHCP.

Appendix B
Proposed Model Validation

In this section, we will discuss about the validation of our proposed measurement model. To calculate nonreciprocal rotation taking the phase of the propagating wave and their interaction with the DUT is very important. In the EM environment, we benchmark the simulated performance based on the proposed mathematical model. Fig. 7(a) shows the simulated Faraday rotation based on deembedding and without deembedding where we observed the maximum rotation at resonance is slightly lower if we do not deembed the metasurface from the free-space regions between the floquet port and DUT. Fig. 7(b) shows the simulation setup with deembedding option active. During the cosimulation, we have taken 377 Ω for the floquet port impedances to mimic the output impedance of horn antenna.

Although deembedding, i.e., isolating the metasurface S-parameters from the composite free-space/metafurface/free-space system, is very important in extracting the Faraday rotation, we did not have accurate fixture and calk it to correctly take the deembedding from antenna to DUT. Besides, calibration up to the DUT plane might be very complicated based on the mathematical modeling discussed here. Our proposed mathematical model requires extraction of four different polarization states (i.e., xx, yy, xy, and yx). Therefore, accurate calibration up to the DUT plane requires all four polarization states be taken into account. In order to simplify the procedure, as previously mentioned we used the SOLT calibration which takes the calibration from the VNA to the antenna port. Fig. 8 shows the test bench setup. Both antennas are placed at a minimum far-field distance from the DUT,

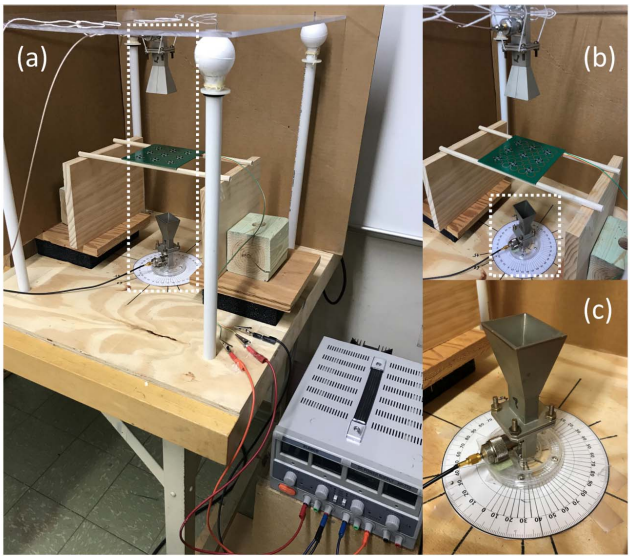

Fig. 8. (a) Test bench setup with mounted horn antennas, one fixed (top) and the other variable (bottom). The metamaterial is placed equidistant between the two antennas in the far-field. The power supply used to bias the gate and drain terminals of transistors in the metamaterial is shown bottom right. (b) Zoomed-in view of dashed section outlined in (a). (c) Zoomed-in view of dashed section outlined in (b) shows the receiving horn antenna mounted on a Lazy Suzan with a protractor used to measure the rotation angle manually with respect to the co-polarized state, for the manual measurement method [23].

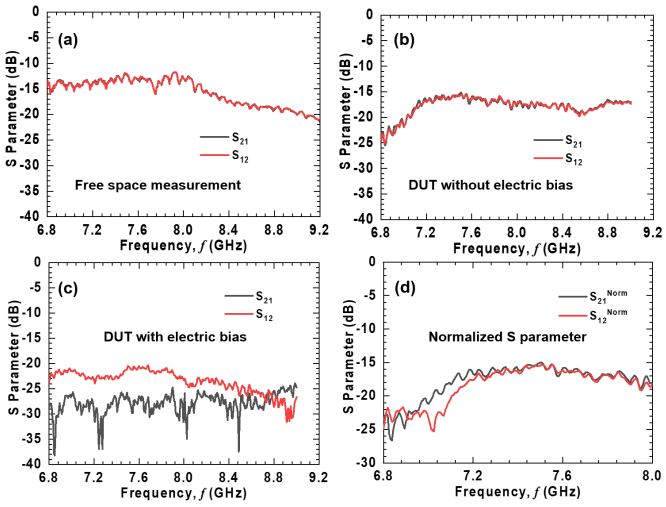

Fig. 9. Measured S_{21} and S_{12} (a) in absence of metasurface, (b) in presence of metasurface without any applied bias condition, and (c) in presence of metasurface with applied bias condition, an example of nonreciprocity. (d) Normalized S parameter from (b) and (c).

which is positioned in the middle. The dimension of the DUT has been calculated based on the antenna beamwidth at that position so that the wave propagates from antenna 1 (2) to antenna 2 (1) only through the DUT. The test bench has been developed based on wood and plastic (low permittivity) to avoid any unwanted reflection.

In order to improve accuracy and validate our proposed model, we computed the S-parameters in different steps. Fig. 9(a) shows the free space measurement where we measure the S_{21} and S_{12} removing the DUT. As expected, we do not observe any nonreciprocal behavior. Fig. 9(b) shows the S-parameter in presence of DUT. However, there is no electrical bias applied and we observe the metasurface itself in absence of bias is reciprocal, hence, the metasurface does not exhibit any Faraday rotation in the absence of bias, as expected. This step helps us to understand the loss due to the meatasurface board. Fig. 9(c) shows when we turn on the bias condition and we observe the nonreciprocal behavior from S parameter in forward and reverse direction. Fig. 9(d) shows normalized S parameter with respect to the nominal condition. We can still take the phase changes into account and extract Faraday rotation based on the proposed model. We have applied similar approaches to calculate all required polarizations. Furthermore, in simulation and in both measurement procedures discussed here, we have taken the same reference plane and distance between the antenna and metasurface to compare/contrast and be consistent.

ACKNOWLEDGMENT

The authors would like to thank Dr. Md. Tanvir Hasan and Ragib Shakil Rafi for helpful discussions and guidance.

REFERENCES

[1] B. Lax, K. Button, K. Button, and K. Button, *Microwave Ferrites and Ferrimagnetics* (Lincoln Laboratory Publications). New York, NY, USA: McGraw-Hill, 1962. [Online]. Available: https://books.google.com/books?id=LAhTAAAAMAAJ

[2] V. Asadchy, M. S. Mirmoosa, A. Díaz-Rubio, S. Fan, and S. A. Tretyakov, "Tutorial on electromagnetic nonreciprocity and its origins," 2020, *arXiv:2001.04848*.

[3] C. Caloz, A. Alù, S. Tretyakov, D. Sounas, K. Achouri, and Z.-L. Deck-Léger, "Electromagnetic nonreciprocity," *Phys. Rev. A, Gen. Phys.*, vol. 10, no. 4, Oct. 2018, Art. no. 047001, doi: 10.1103/PhysRevApplied.10.047001.

[4] C. L. Hogan, "The ferromagnetic Faraday effect at microwave frequencies and its applications: The microwave gyrator," *Bell Syst. Tech. J.*, vol. 31, no. 1, pp. 1–31, Jan. 1952.

[5] C. Caloz and T. Itoh, *Electromagnetic Metamaterials: Transmission Line Theory and Microwave Applications*. Hoboken, NJ, USA: Wiley, 2005.

[6] T. Kodera, D. L. Sounas, and C. Caloz, "Artificial Faraday rotation using a ring metamaterial structure without static magnetic field," *Appl. Phys. Lett.*, vol. 99, no. 3, 2011, Art. no. 031114, doi: 10.1063/1.3615688.

[7] D. L. Sounas *et al.*, "Faraday rotation in magnetically biased graphene at microwave frequencies," *Appl. Phys. Lett.*, vol. 102, no. 19, 2013, Art. no. 191901, doi: 10.1063/1.4804437.

[8] G. Lavigne, T. Kodera, and C. Caloz, "'Perfect' faraday-rotation metasurface," in *Proc. 14th Int. Congr. Artif. Mater. Novel Wave Phenomena (Metamaterials)*, 2020, pp. 156–158.

[9] T. Kodera, D. L. Sounas, and C. Caloz, "Switchable magnetless nonreciprocal metamaterial (MNM) and its application to a switchable Faraday rotation metasurface," *IEEE Antennas Wireless Propag. Lett.*, vol. 11, pp. 1454–1457, 2012.

[10] N. Parsa, M. R. Gasper, B. C. Amacher, and R. C. Toonen, "Millimeter-wave Faraday rotation from ferromagnetic nanowires," *IEEE Trans. Nanotechnol.*, vol. 18, pp. 839–844, 2019.

[11] A. Nagulu, N. Reiskarimian, and H. Krishnaswamy, "Non-reciprocal electronics based on temporal modulation," *Nature Electron.*, vol. 3, no. 5, pp. 241–250, 2020, doi: 10.1038/s41928-020-0400-5.

[12] A. Kord, D. L. Sounas, and A. Alù, "Microwave nonreciprocity," *Proc. IEEE*, vol. 108, no. 10, pp. 1728–1758, Oct. 2020.

[13] T. Kodera and C. Caloz, "Unidirectional loop metamaterials (ULM) as magnetless artificial ferrimagnetic materials: Principles and applications," *IEEE Antennas Wireless Propag. Lett.*, vol. 17, no. 11, pp. 1943–1947, Nov. 2018.

[14] S. J. Orfanidis, *Electromagnetic Waves and Antennas*. New Brunswick, NJ, USA: Rutgers Univ. Press, 2016. [Online]. Available: https://www.ece.rutgers.edu/~orfanidi/ewa/

[15] S. Poddar, "Design and analysis of fully-electronic magnet-free non-reciprocal metamaterial," M.S. thesis, Dept. Elect. Eng., Univ. Wisconsin-Milwaukee, Milwaukee, WI, USA, 2020. [Online]. Available: https://dc.uwm.edu/etd/2578
[16] S. V. Kutsaev, A. E. Krasnok, S. N. Romanenko, A. Y. Smirnov, K. Taletski, and V. Yakovlev, "Up-and-coming advances in optical and microwave nonreciprocity: From classical to quantum realm," Tech. Rep., 2020, doi: 10.1002/adpr.202000104.
[17] C. Caloz, A. Alù, S. Tretyakov, D. Sounas, K. Achouri, and Z.-L. Deck-Léger, "What is nonreciprocity—Part II," 2018, *arXiv:1804.00238*.
[18] C. Caloz and A. Sihvola, "Electromagnetic chirality," Tech. Rep., 2019, doi: 10.48550/arXiv.1903.09087.
[19] D. Floess *et al.*, "Tunable and switchable polarization rotation with non-reciprocal plasmonic thin films at designated wavelengths," *Light, Sci. Appl.*, vol. 4, no. 5, p. e284, May 2015, doi: 10.1038/lsa.2015.57.
[20] I. Lindell, A. Sihvola, S. Tretyakov, and A. Viitanen, *Electromagnetic Waves in Chiral and Bi-Isotropic Media*. Norwood, MA, USA: Artech House, 1994.
[21] S. Poddar, R. S. Rafi, and M. T. Hasan, "Analytical modeling of electromagnetic rotation in nonreciprocal media," 2022, *arXiv:2205.03560*.
[22] S. Poddar, M. T. Hasan, and R. S. Rafi, "Computational approach of designing magnetfree nonreciprocal metamaterial," *Prog. Electromagn. Res. C*, vol. 121, pp. 197–206, 2022.
[23] S. Poddar, A. M. Holmes, and G. W. Hanson, "Design and analysis of an electronically tunable magnet-free non-reciprocal metamaterial," *IEEE Trans. Antennas Propag.*, vol. 70, no. 8, pp. 7311–7315, Aug. 2022.
[24] C. Menzel, C. Rockstuhl, and F. L. Lederer, "Advanced Jones calculus for the classification of periodic metamaterials," *Phys. Rev. A, Gen. Phys.*, vol. 82, Nov. 2010, Art. no. 053811.

Swadesh Poddar (Member, IEEE) was born in Khulna, Bangladesh, in 1989. He received the B.Sc. degree in electronics and communication engineering from Khulna University, Khulna, in 2011, and the M.S. degree in electrical engineering from the University of Wisconsin–Milwaukee, Milwaukee, WI, USA, in 2020.

From 2011 to 2015, he worked as a QoS Engineer at Banglalink, Vimpelcom Ltd., Dhaka, Bangladesh, and from 2016 to 2018, he worked as a Technical Consultant in Bangabandhu Satellite Launching Project 1. He is currently working as a Design Engineer at Qorvo, Inc., Apopka, FL, USA. His research interests include nonreciprocal metamaterial, antenna, and radio frequency (RF) systems design.

Alexander M. Holmes (Member, IEEE) was born in Milwaukee, WI, USA, in 1995. He received the B.S. degree in physics from the University of Wisconsin–Stevens Point, Stevens Point, WI, USA, in 2017, and the Ph.D. degree in electrical engineering from the University of Wisconsin–Milwaukee, Milwaukee, WI, in 2022.

He currently works with the Airborne Radar Electronics Department, Raytheon Intelligence and Space, El Segundo, CA, USA, as an radio frequency (RF) Transmit/Receive Module Engineer. His research interests include nonreciprocal electromagnetic (EM) wave phenomena in layered media, integrated transmission lines, waveguides, and antennas.

George W. Hanson (Fellow, IEEE) was born in Glen Ridge, NJ, USA, in 1963. He received the B.S.E.E. degree from Lehigh University, Bethlehem, PA, USA, in 1986, the M.S.E.E. degree from Southern Methodist University, Dallas, TX, USA, in 1988, and the Ph.D. degree from Michigan State University, East Lansing, MI, USA, in 1991.

From 1986 to 1988, he was a Development Engineer with General Dynamics, Fort Worth, TX, USA, where he worked on radar simulators. From 1988 to 1991, he was a Research and Teaching Assistant at the Department of Electrical Engineering, Michigan State University. He is currently a Professor Emeritus of electrical engineering and computer science with the University of Wisconsin–Milwaukee, Milwaukee, WI, USA. He is the coauthor of the book *Operator Theory for Electromagnetics: An Introduction* (New York: Springer, 2002) and the author of *Fundamentals of Nanoelectronics* (NJ, USA: Prentice-Hall, 2007). His research interests include nanoelectromagnetics, quantum optics, mathematical methods in electromagnetics (EMs), and EM wave phenomena in layered media.

Dr. Hanson is a member of International Union of Radio Science (URSI) Commission B, Sigma Xi, and Eta Kappa Nu. In 2006, he received the S. A. Schelkunoff Best Paper Award from the IEEE Antennas and Propagation Society. He was an Associate Editor for the IEEE TRANSACTIONS ON ANTENNAS AND PROPAGATION from 2002 to 2007.